Second Harmonic Generation Based on Strong Field Enhancement in Metallic Nanostructured Surface

Kitsakorn LOCHAROENRAT*

Physics Department, King Mongkut's Institute of Technology Ladkrabang, Bangkok 10520, Thailand

Although absorption is still the primary optical property of interest, other spectroscopic techniques including optical second harmonic generation (SHG) are also used to understand anisotropic nature of nanomaterials. Benefit of SHG technique as compared with linear optical approach is that SH response is the most sensitive to surface potential changes and SH intensity mainly comes from surface/interface layers. This article reports that optical absorption spectra due to surface plasmon modes of metallic nanowires exhibit strong anisotropic absorption. Maxwell-Garnett simulation cannot fit with experimental results because of wire sizes much larger than wavelength of light, whereas finite-difference time-domain calculation can fit well with experimental findings in terms of position of photon energy of absorption peak with respect to polarization conditions.

Keywords: finite-difference time-domain, Maxwell-Garnet model, nanowires, second harmonic generation, surface plasmon.

1. INTRODUCTION

In solid state materials there are electrons localized close to positive ions and free electrons contributing to electrical conductivity. Interaction of electrons with materials is reflected in dielectric function. We can also describe the effect of free electrons in the dielectric function. Lorentz model describes the dielectric properties of insulators most simply, in which electrons are bound to positive ions. Equation of motion of an electron in an oscillating electric field of frequency ω is:

$$m\left[\frac{d^2x}{dt^2} + \Gamma_0 \frac{dx}{dt} + \omega_0^2 x\right] = qE \; ; \tag{1}$$

$$m\left[\frac{d^2x}{dt^2} + \Gamma_0 \tau \frac{dx}{dt} + \omega_0^2 x\right] = qE_0 e^{-i\omega t} \; . \tag{2}$$

The m is free electron mass, x is displacement, and Γ_0 is damping constant. The τ is time interval between one scattering and another of free electron, and is normally about 10 fs. The ω_0 is frequency of a transverse wave and q is electric charge. The E is electric filed giving rise to polarization.

When we assume a solution of the form,

$$x = x_0 e^{-i\omega t} \; . \tag{3}$$

The x_0 is found as,

$$x_0 = \frac{qE_0}{m(\omega_0^2 - \omega^2 - i\omega\Gamma_0)} \; . \tag{4}$$

In metals and semiconductors (Drude Model), if we suppose that there is no restoring force applied to free electron, substituting ω_0 is equal to zero. Equation (2) is modified as,

$$m*\left[\frac{d^2x}{dt^2} + \tau^{-1} \frac{dx}{dt}\right] = qE_0 e^{-i\omega t} \; . \tag{5}$$

The $m*$ is effective mass. Dielectric function of this material of volume fraction V is,

$$\varepsilon = \varepsilon_0 - \frac{Ne^2}{m*V\omega(\omega + i\tau^{-1})} \; . \tag{6}$$

The N is electron concentration.

On one hand, when $\omega \sim 0$, equation (6) becomes,

$$\varepsilon = \varepsilon_0 + i\frac{Ne^2\tau}{m*V\omega} \; . \tag{7}$$

If electrical conductivity is defined as,

$$\sigma = \frac{Ne^2\tau}{m*V} \tag{8}$$

equation (7) reads,

$$\varepsilon = \varepsilon_0 + i\frac{\sigma}{\omega} \; . \tag{9}$$

On the other hand, when $\omega >> \tau^{-1}$, equation (6) becomes,

$$\varepsilon = \varepsilon_0 - \frac{Ne^2}{m*V\omega^2} \; . \tag{10}$$

If

$$\omega_p = \sqrt{\frac{Ne^2}{m*\varepsilon_0 V}} \tag{11}$$

one reads:

$$\varepsilon = \varepsilon_0\left[1 - \frac{\omega_p^2}{\omega^2}\right] . \tag{12}$$

The ω_p is plasma frequency and $\hbar\omega$ is located in a visible or ultraviolet photon energy region. Below this energy level, real metal behave like an ideal metal and its optical reflectivity is close to 1. On the other hand, above this energy regime, free carriers in metal cannot follow the variation of electric field and thus electromagnetic wave can

---
*Corresponding author. Tel.: +66-2329-8000, fax: +66-2329-8412.
E-mail address: *klkitsak@kmitl.ac.th* (K. Locharoenrat)

penetrate and propagates freely into metal. If $\omega = \omega_p$, $\varepsilon = 0$ according to equation (12) and wavelength of light becomes infinite. This resonance condition corresponds to a collective excitation called plasmon [1–4]. In other words, plasmon oscillation or coupling of electromagnetic field with metals and semiconductors can affect theirs electron subsystem [5–10]. When external field is changed, the electron subsystem can oscillate in the field leading to surface charges along the field.

On the other hand, optical second harmonic generation (SHG) appears to be one of the most attractive as a tool for metal surface study due to a main reason of being highly surface-specific for any solid-state materials [11–15]. When electron is in ideally parabolic potential, it makes a linear optical response to external electric field. In contrary, if electron is in non-parabolic potential, its response to the external field is nonlinear. In nonlinear optical effect, magnitude of generated polarization is not proportional to that of incident electric field.

Nonlinear polarization as a function of incident electric field can be written as,

$$\vec{P} = \varepsilon_0 \left[\chi^1 \vec{E}^1 + \chi^2 \vec{E}^2 + \chi^3 \vec{E}^3 + ... \right] ; \qquad (13)$$

$$\vec{P} = \vec{P}^1 + \vec{P}^2 \vec{P}^2 + ... ; \qquad (14)$$

$$\vec{P} = \vec{P}^1 + \vec{P}^{NL} . \qquad (15)$$

The χ^2 and χ^3 is nonlinear susceptibility tensor, whereas $\vec{P}^{NL}$ is nonlinear polarization.

The ith component of second order nonlinear polarization is,

$$P_i^2(\omega_i) = \sum_{jk} \varepsilon_0 \chi_{ijk}^2(-\omega_i, \omega_j, \omega_k) E_j(\omega_j) E_k(\omega_k) , \qquad (16)$$

where $\vec{P}(\omega_i) \propto e^{-i\omega_i t}$ and $\vec{E}(\omega_j) \propto e^{-i\omega_j t}$.

The nonlinear optical response of material enables us to perform a surface sensitive spectroscopy including optical second harmonic spectroscopy of solid surfaces. Second-order process, such as SHG ($\omega_2 = 2\omega_1$) is a phenomenon in which polarization

$$P = \chi^2 E^2 \qquad (17)$$

induced by incident electric field $E \propto \exp(-i\omega t)$, radiates a light of double frequency $E \propto \exp(-2i\omega t)$. The SHG occurs in a medium whose structure lacks inversion symmetry like structures near nanowire surfaces as shown in Fig. 1.
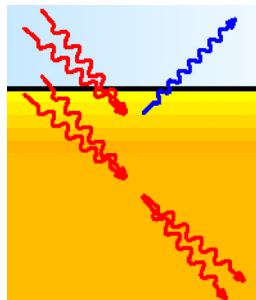
Fig. 1. The double photon enegrgy (blue wavy arrows) produced by collision of single photon enegrgy (red wavy arrows)

Since the second-order responses of our samples depend sensitively on the detailed structure of the samples, they result in their nonlinear responses [12, 13]. In order to see how sensitive the SHG technique is, this article focuses on SHG as a noninvasive monitor of plasmon oscillation in metallic nanowires.

2. THEORETICAL MODEL AND ANALYSIS

This article presents a simple model for calculation of absorption spectra, Maxwell-Garnett model [16], in which objects of short wire axes b are assumed to be smaller than wavelength of incident light (Fig. 2). By making aspect ratio of a/b to be infinity, one can treat ellipsoid-shape metal as metallic nanowire.

In this quasi-static regime, we are able to calculate the field distributions to metallic nanowires placed in an external uniform field. In metallic nanowires, the applied static electric field induces a dipole moment and polarizability α is therefore defined through [1, 2]:

$$\alpha = \frac{V}{3Q} \left[\frac{\varepsilon_m(\omega_p) - \varepsilon_0}{\varepsilon_m(\omega_p) + (Q^{-1} - 1)\varepsilon_0} \right] , \qquad (18)$$

where ε_m and ε_0 are dielectric constant of metallic nanowires and environment, respectively. The ω_p denotes resonance frequency. The V is volume fraction. The Q is depolarization factor depending on ratio of long wire axes a/short wire axes b. The electric polarizability α in equation (18) can show a resonance behavior when a real part of denominator $\mathrm{Re}\{\varepsilon_m(\omega_p) + (Q^1 - 1)\varepsilon_0\}$ becomes zero, which is a case for $\mathrm{Re}\{\varepsilon_m(\omega_p)\} = \varepsilon_0 - \varepsilon_0 Q^{-1}$.
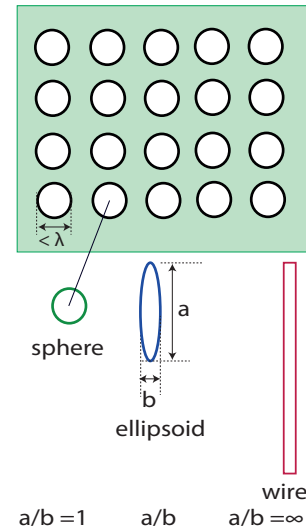
Fig. 2. Composite particles in host medium. The a and b are long and short axes of metallic nanowires, respectively

From equation (18), surface plasmon mode of metallic nanowires is dependent of dielectric constant ε, resonance frequency ω_p, and depolarization factor Q. First, when depolarization factor Q is in between 0 and 1, surface plasmon excitation exists because their real part $\mathrm{Re}\{\varepsilon_m(\omega_p)\}$ fulfills resonance condition $\mathrm{Re}\{\varepsilon_m(\omega_p) + (Q^{-1} - 1)\varepsilon_0\}$ at visible light. Second, resonance frequency ω_p is dependent of depolarization factor Q and dielectric constant of environment ε_0. Then, one can tune plasmon excitation via

Q and ε_0. That is, when Q and ε_0 are enhanced, plasmon maxima tend to be red-shift. A defined tuning of ω_p over a whole visible spectrum region is then possible. Last, imaginary part of $\varepsilon(\omega)$ can predict a tendency of spectral width of surface plasmon profile. When imaginary part of $\varepsilon(\omega)$ is reduced (Table 1 and Fig. 3), the profile becomes sharp.

Table 1. Dielectric constant of different metals

Metals	ε_m ($\lambda = 1064$ nm)	ε_m ($\lambda = 532$ nm)
Silver	$-58.14 + i0.61$	$-11.78 + i0.37$
Gold	$-48.24 + i3.59$	$-4.71 + i2.42$
Copper	$-49.13 + i4.91$	$-5.50 + i5.76$
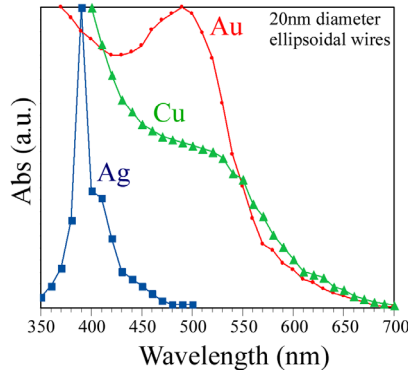
Fig. 3. Absorption spectra of metallic nanowires calculated by finite-difference time-domain method

Since the electrostatic application as explained in Maxwell-Garnet model accounts for a homogeneous distribution of electromagnetic field entirely the metallic wire volume, the more realistic methods, namely, finite-difference time-domain method (FDTD) needs to be applied [17, 18]. The FDTD calculation can solve an entirely set of Maxwell's equations for coupling of light with any shape and size of metallic nanowires. Maxwell's curl equations accompanied with dielectric function of metals by Drude model are generally valid for dielectric materials, and their electromagnetic fields are able to solve simultaneously in time and space.

For practical application of FDTD the commercial software, developed by Lumerical Inc. from Canada, is exploited [19]. This program simulates different conditions for coupling of light with metallic nanowire shape and size, and gives outcome of their absorption spectra and field distributions. Input parameters for FDTD programs are: shape of object, material of interest, cell size, and incident angle of incident light. Advantage of FDTD technique is that we can use very tiny cubic cells to cover all surfaces of interest. This guarantees an accuracy of field distribution over metallic nanowires. Some drawbrack of this technique is that calculation time rises with increasing a number of cell. For example, one simulation time is aproximately 500 fs as shown in Fig. 4. In addition, the fine discretization in finite differencing increases the rounding off error as well. Hence, a balance between accuracy and round off error needs to be maintained in FDTD method.
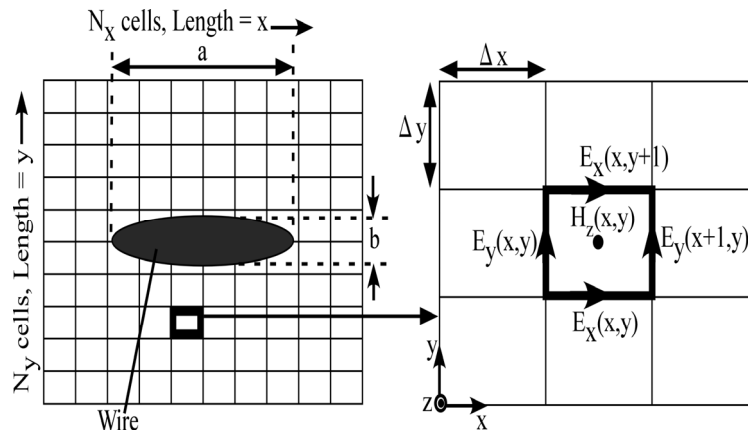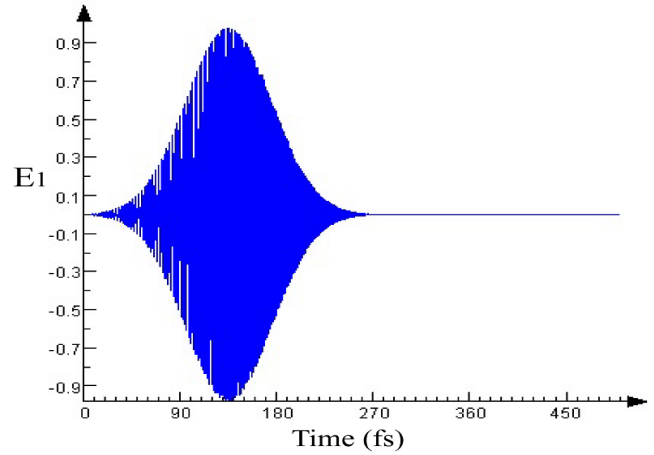
Fig. 4. FDTDSmain simulation time is about 500 fs

The simulation has converged when the component of electric field has decayed to zero before the end of of the simulation time. The intensity of the total field is calculated and normalized to that of the incident field. For all simulations, absorbing boundary conditions based on the perfectly matched layer approximation are applied.

Fig. 5 shows a model of metallic nanowires used as object for FDTD calculation. The nanowires are surrounded by 2-D unit cell with a grid size of 0.1 nm × 0.1 nm. The geometrical parameters for the long wire axes (a) is 200 nm and for the short axes (b) is 20 nm. These calculated parameters provide an aspect ratio (a/b) of 10 corresponding well with the aspect ratio obtained from

Fig. 5. Coordination system for finite-difference time-domain simulation. The a and b are long and short wire axes of metallic nanowires, respectively. The aspect ratio is a/b related to geometrical effecting on the surface plasmon mode

our previous experimental data of fabricated nanowires [9]. By considering *x*-polarized light traveling in the forward *y*-direction and *x*-polarized light traveling in the forward *y*-direction, the three electromagnetic field components $E_x(x,y,t)$, $E_y(x,y,t)$, and $H_z(x,y,t)$ for each polarization direction can be calculated. Calculated absorption spectra agree well with typical experimentally obtained absorption spectra partly due to surface plasmon modes [9]. With increasing the short wire axes *b* at the same aspect ratio *a/b*, the absorption spectra shift to lower photon energy region. This is in agreement with the fact that retardation effect, which means external non-uniform field around metallic nanowires, has important on plasmon maxima.

On the other hand, surface plasmon mode do not only lead to a consequence for the absorption spectra, but they also lead to field enhancement in second harmonic generation (SHG) process induced by a broken symmetry. Let us consider a potential of electron of mass *m* along the coordinate *z*,

$$\frac{V}{m}(z)=0.5\omega_0^2 z^2 + a_3 z^3 + a_4 z^4 + ... \quad . \tag{19}$$

If this potential is symmetric with respect to the point $z = 0$, we have $a_{2n+1} = 0$. In contrast, if it is asymetric, the equation of motion of the electron will be,

$$m\frac{d^2z}{dt^2}+m\omega_0^2 z + 3a_3 z^2 + 4a_4 z^3 + ... = Fe^{-i\omega t} . \tag{20}$$

The solution of this equation to the first order by the perturbation theory is,

$$z = z^{(0)} + z^{(1)}, \tag{21}$$

where

$$z^{(0)} = \frac{F}{m(\omega_0^2 - \omega^2)} e^{-i\omega t} \tag{22}$$

and

$$z^{(1)} = \frac{-3a_3}{m(\omega_0^2 - 4\omega^2)} \frac{F^2}{m^2(\omega_0^2-\omega^2)^2} e^{-2i\omega t} . \tag{23}$$

Therefore, this proves that SHG is a phenomenon in which a polarization induced by incident electric field

$E \propto \exp(-i\omega t)$, radiates a light of double frequency $E \propto \exp(-2i\omega t)$.

In terms of the field enhancement in second harmonic generation (SHG) process, it can be defined by [14, 15]:

$$L = \left|\vec{E}\right|/\left|\vec{E}_o\right| = L(\vec{r}, \omega) \tag{24}$$

where $\vec{E}$ denotes optical field and $\vec{E}_o$ denotes incoming field. In equation (24), the field enhancement *L* is mainly determined by the field at position $\vec{r}$ and at resonance frequency ω_p of the exciting light. This expression depends on polarization conditions with respect to metallic nanowire surfaces as well. For polarization parallel to the nanowire axes, the external field is continuous across their surfaces. Then the enhancement is possible for a resonant excitation of the surface plasmon. For polarization perpendicular to the nanowire axes, the enhancement is also possible due to contribution of corner effect around their edges as shown in Fig. 6. The field near circular wires in Fig. 6 (top), which are highly symmetric, is homogeneous on the entire surface. A strong field in the single wires can be related to oscillating polarization charges with positive charges on the one side of the wires and negative charges on the other side. Polarization charges of opposite signs are confined between gap and they results in the electric field enhancements.

The polarization charge distributions for non-regular wires, which are less symmetric, are different from the circular ones. The charges are mainly concentrated around the corners. Namely, on the left side of the single square wires in Fig. 6 (middle), the charge distributions with the same sign (minus charges) are accumulated at the top (one minus charge at top left) and bottom (another minus charge at bottom left) of the corners. On the other hand, plus charges at the upper and lower corners are located on the right side of the single wires. These charges topology of the opposite signs (positive and negative charges) accumulated around the corners lead to a dipole-like field distribution between gap and result in the strong electric fields. Reducing the wire symmetry from square wires in Fig. 6 (middle) to triangular wires in Fig. 6 (bottom)
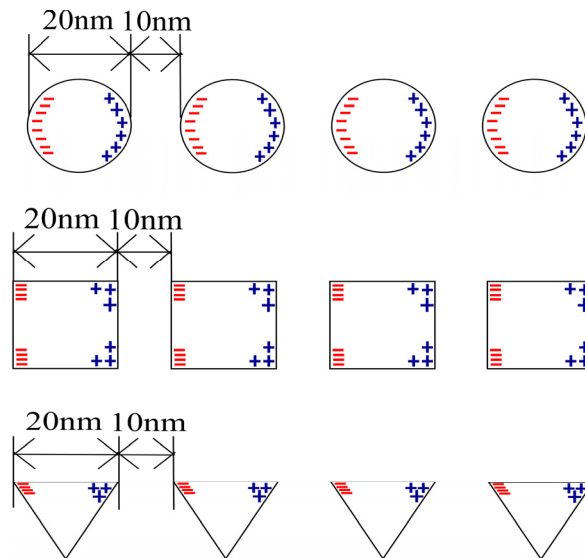
Fig. 6. Field ditributions of different cross-section shapes from metallic nanowires

increases the sharpness of corners, leading to a strongly confined charge and a dipolar interaction. The sharper the corner, the more confined the surface charges and the stronger the resulting field enhancements.

The electric field enhancements were found to depend on the asymmetric structure of the wires especially for noncircular shapes (triangular and square wires). Therefore, we suggest that the lightning rod effect must be taken into account for an accurate description of the field distribution in real nanowire structures.

Electric field enhancement on SHG process also can be demonstrated by FDTD simulation via plasmon maxima in metallic nanowires [20, 21]. Field enhancement exists near metallic nanowires for parallel polarization conditions. The electric field enhancement is dominant when a periodicity of the metallic nanowires is reduced. There are two contributions existed according to the decrease of the periodicity. In short distance, short-range interactions between neighboring wires induce near-field coupling and create highly sensitive plasmons confined to metal boundaries. In contrast, when the periodicity exceeds the range of near-field coupling, far-field interactions prevail among wires. This mechanism can be explained by using a dipole-dipole interaction model. Dipole field in an individual wire induces the dipoles in the neighboring wires by distorting the neighbor's electron cloud and it leads to the formation of localized surface plasmons and then results in local electric field enhancement.

3. CONCLUSIONS

This article explains surface plasmon modes in general and concepts of second harmonic generation. A simple analytical method based on Maxwell-Garnett model is then presented for calculation of absorption spectra. A numerical method, finite-difference time-domain is then shown and this allows one to accurately calculate plasmon maxima in metallic nanowires. It is found that Maxwell-Garnett simulation do not fit with experimental results due to wire sizes much larger than wavelength of incident light, however, finite-difference time-domain calculation is in agreement well with the findings because finite-difference time-domain calculation can solve an entirely set of Maxwell's equations for coupling of light with any shape and size of metallic nanowires.

REFERENCES

1. **Gaponenko, S. V.** Introduction to Nanophotonics. Cambridge, Now York, 2010: pp. 130 – 140.
    http://dx.doi.org/10.1017/CBO9780511750502

2. **Jahns, J., Helfert, S.** Introduction to Micro- and Nanooptics. Wiley, New York, 2012: pp. 215 – 229.

3. **Zangwill, A.** Physics at Surfaces. Cambridge, New York, 2008: pp. 25 – 100.

4. **Samorjai, G.** Chemistry in Two Dimensions. Ithaca, New York, 2011: pp. 50 – 125.

5. **Gutierrez, F. A., Salas, C., Jouin, H.** Bulk Plasmon Induced Ion Neutralization Near Metal Surfaces *Surface Science* 606 (15 – 16) 2012: pp. 1293 – 1297.

6. **Yeshchenko, O. A., Bondarchuk, I. S., Dmitruk, I. M., Kotko, A. V.** Temperature Dependence of Surface Plasmon Resonance in Gold Nanoparticle *Surface Science* 608 2013: pp. 275 – 281.

7. **Ning, J., Nagata, K., Ainai, A., Hasegawa, H., Kano, H.** Detection of Influenza Virus with Specific Subtype by Using Localized Surface Plasmons Excited on a Flat Metal Surface *Japanese Journal of Applied Physics* 52 2013: pp. 82402 – 82405.

8. **Mott, D., Lee, J. D., Thuy, N., Aoki, Y., Singh, P., Maenosono, S.** A Study on the Plasmonic Properties of Silver Core Gold Shell Nanoparticles *Japanese Journal of Applied Physics* 50 2011: pp. 65004 – 65011.

9. **Locharoenrat, K., Sano, H., Mizutani, G.** Phenomenological Studies of Optical Properties of Cu Nanowires *Science and Technology of Advanced Materials* 8 2007: pp. 277 – 281.
    http://dx.doi.org/10.1016/j.stam.2007.02.001

10. **Wunderlich, S., Peschel, U.** Plasmonic Enhancement of Second Harmonic Generation on Metal Coated Nanoparticles *Optic Express* 21 (16) 2013: pp. 18611 – 18623.

11. **Dounce, S. M., Yang, M., Dai, H. L.** Physisorption on Metal Surface Probed by Surface State Resonant Second Harmonic Generation *Surface Science* 565 (1) 2004: pp. 27 – 36.

12. **Locharoenrat, K., Sano, H., Mizutani, G.** Rotational Anisotropy in Second Harmonic Intensity from Copper Nanowire Arrays on the NaCl (110) Substrates *Journal of Luminescence* 128 2008: pp. 824 – 827.
    http://dx.doi.org/10.1016/j.jlumin.2007.11.056

13. **Locharoenrat, K., Sano, H., Mizutani, G.** Second Harmonic Spectroscopy of Copper Nanowire Arrays of on the (110) Faceted Faces of NaCl Crystals *Journal of Physics: Conference Series* 100 2008: pp. 52050 – 52053.

14. **Bloembergen, N.** Nonlinear Optics. Wiley, New York, 2005: pp. 27 – 38.

15. **Shen, Y. R.** The Principle of Nonlinear Optics. Wiley, New York, 2004: pp. 3 – 32.

16. **Garnett, J. C. M.** Colours in Metal Glasses and in Metallic Films *Philos. Trans. R. Soc. London Ser. A* 203 1904: pp. 385 – 420.
    http://dx.doi.org/10.1098/rsta.1904.0024

17. **Taflove, A.** 'Computational Electrodynamics: the Finite-difference Time-domain Method. Artech House, Boston, 2005: pp. 95 – 115.

18. **Sullivan, D. M.** Electromagnetic Simulation Using the FDTD Method. IEEE, New York, 2005: pp. 42 – 77.

19. FDTD Solutions v8.7.4.
    https://www.lumerical.com/downloads/

20. **Locharoenrat, K., Mizutani, G.** Characterization, Optical and Theoretical Investigation of Arrays of the Metallic Nanowires Fabricated by a Shadow Deposition Method *Advanced Materials Research* 652 2013: pp. 622 – 623.

21. **Locharoenrat, K., Sano, H., Mizutani, G.** Field Enhancement in Arrays of Copper Nanowires Investigated by the Finite-difference Time-domain Method *Surface and Interface Analysis* 40 2008: pp. 1635 – 1638.